Electro-optical switching between polariton and cavity lasing in an InGaAs quantum well microcavity

Matthias Amthor,[1,*] Sebastian Weißenseel,[1] Julian Fischer,[1] Martin Kamp,[1] Christian Schneider,[1] and Sven Höfling,[1,2]

[1]*Technische Physik, Physikalisches Institut and Wilhelm Conrad Röntgen-Research Center for Complex MaterialSystems, Universität Würzburg, Am Hubland, D-97074, Würzburg, Germany*
[2]*SUPA, School of Physics and Astronomy, University of St Andrews, St Andrews, KY16 9SS, UK*
[*]*Matthias.amthor@physik.uni-wuerzburg.de*

Abstract: We report on the condensation of microcavity exciton polaritons under optical excitation in a microcavity with four embedded InGaAs quantum wells. The polariton laser is characterized by a distinct non-linearity in the input-output-characteristics, which is accompanied by a drop of the emission linewidth indicating temporal coherence and a characteristic persisting emission blueshift with increased particle density. The temporal coherence of the device at threshold is underlined by a characteristic drop of the second order coherence function to a value close to 1. Furthermore an external electric field is used to switch between polariton regime, polariton condensate and photon lasing.

OCIS codes: (250.5590) Quantum-well, -wire and -dot devices; (190.5890) Scattering, stimulated; (230.5750) Resonators; (140.3948) Microcavity devices.

References and links

1. C. Weisbuch, M. Nishioka, A. Ishikawa, and Y. Arakawa, "Observation of the coupled exciton-photon mode splitting in a semiconductor quantum microcavity," Phys. Rev. Lett. **69**(23), 3314–3317 (1992).
2. H. Deng, G. Weihs, D. Snoke, J. Bloch, and Y. Yamamoto, "Polariton lasing vs. photon lasing in a semiconductor microcavity," Proc. Natl. Acad. Sci. U.S.A. **100**(26), 15318–15323 (2003).
3. E. Kammann, H. Ohadi, M. Maragkou, A. V. Kavokin, and P. G. Lagoudakis, "Crossover from photon to exciton-polariton lasing," New J. Phys. **14**(10), 105003 (2012).
4. H. Deng, G. Weihs, C. Santori, J. Bloch, and Y. Yamamoto, "Condensation of semiconductor microcavity exciton polaritons," Science **298**(5591), 199–202 (2002).
5. J. Kasprzak, M. Richard, S. Kundermann, A. Baas, P. Jeambrun, J. M. J. Keeling, F. M. Marchetti, M. H. Szymańska, R. André, J. L. Staehli, V. Savona, P. B. Littlewood, B. Deveaud, and S. Dang, "Bose-Einstein condensation of exciton polaritons," Nature **443**(7110), 409–414 (2006).
6. S. Christopoulos, G. B. H. von Högersthal, A. J. D. Grundy, P. G. Lagoudakis, A. V. Kavokin, J. J. Baumberg, G. Christmann, R. Butté, E. Feltin, J.-F. Carlin, and N. Grandjean, "Room-temperature polariton lasing in semiconductor microcavities," Phys. Rev. Lett. **98**(12), 126405 (2007).
7. S. Kéna-Cohen and S. R. Forrest, "Room-temperature polariton lasing in an organic single-crystal microcavity," Nat. Photonics **4**(6), 371–375 (2010).
8. J. D. Plumhof, T. Stöferle, L. Mai, U. Scherf, and R. F. Mahrt, "Room-temperature Bose-Einstein condensation of cavity exciton-polaritons in a polymer," Nat. Mater. **13**(3), 247–252 (2013).
9. K. S. Daskalakis, S. A. Maier, R. Murray, and S. Kéna-Cohen, "Nonlinear interactions in an organic polariton condensate," Nat. Mater. **13**(3), 271–278 (2014).
10. S. I. Tsintzos, N. T. Pelekanos, G. Konstantinidis, Z. Hatzopoulos, and P. G. Savvidis, "A GaAs polariton light-emitting diode operating near room temperature," Nature **453**(7193), 372–375 (2008).
11. C. Schneider, A. Rahimi-Iman, N. Y. Kim, J. Fischer, I. G. Savenko, M. Amthor, M. Lermer, A. Wolf, L. Worschech, V. D. Kulakovskii, I. A. Shelykh, M. Kamp, S. Reitzenstein, A. Forchel, Y. Yamamoto, and S. Höfling, "An electrically pumped polariton laser," Nature **497**(7449), 348–352 (2013).
12. P. Bhattacharya, B. Xiao, A. Das, S. Bhowmick, and J. Heo, "Solid state electrically injected exciton-polariton laser," Phys. Rev. Lett. **110**(20), 206403 (2013).
13. C. Monier, A. Freundlich, and M. F. Vilela, "Oscillator strength of excitons in InGaAs/GaAs quantum wells in the presence of a large electric field," J. Appl. Phys. **85**(5), 2713–2718 (1999).

#224863 - $15.00 USD Received 15 Oct 2014; revised 11 Nov 2014; accepted 11 Nov 2014; published 8 Dec 2014

14. H. Yu, C. Roberts, and R. Murray, "Influence of indium segregation on the emission from InGaAs/GaAs quantum wells," Appl. Phys. Lett. **66**(17), 2253–2255 (1995).
15. J. L. Sánchez-Rojas, A. Sacedón, F. González-Sanz, E. Calleja, and E. Muñoz, "Dependence on the In concentration of the piezoelectric field in (111)B InGaAs/GaAs strained heterostructures," Appl. Phys. Lett. **65**(16), 2042–2044 (1994).
16. N.J. Traynor, M.J. Snelling, R.T. Harley, R.J. Warburton, and M. Hopkinson, "Investigation of g-factors Zeeman splittings, exchange interactions and field-dependent spin relaxation in III-V quantum wells," Surface Science **361/362**, 435–438 (1996).
17. I. A. Shelykh, A. V. Kavokin, Y. G. Rubo, T. C. H. Liew, and G. Malpuech, "Polariton polarization-sensitive phenomena in planar semiconductor microcavities," Semicond. Sci. Technol. **25**(1), 013001 (2010).
18. P. G. Savvidis, J. J. Baumberg, R. M. Stevenson, M. S. Skolnick, D. M. Whittaker, and J. S. Roberts, "Angle-resonant stimulated polariton amplifier," Phys. Rev. Lett. **84**(7), 1547–1550 (2000).
19. R. M. Stevenson, V. N. Astratov, M. S. Skolnick, D. M. Whittaker, M. Emam-Ismail, A. I. Tartakovskii, P. G. Savvidis, J. J. Baumberg, and J. S. Roberts, "Continuous wave observation of massive polariton redistribution by stimulated scattering in semiconductor microcavities," Phys. Rev. Lett. **85**(17), 3680–3683 (2000).
20. A. Kavokin, J. J. Baumberg, G. Malpuech, and F. P. Laussy, *Microcavities* (Oxford University Press, 2007).
21. M. Amthor, T. C. H. Liew, C. Metzger, S. Brodbeck, L. Worschech, M.Kamp, I. A. Shelykh, A.V. Kavokin, C. Schneider, and S. Höfling, "Optical bistability in electrically driven polariton condensates," submitted.
22. E. Wertz, L. Ferrier, D. D. Solnyshkov, P. Senellart, D. Bajoni, A. Miard, A. Lemaitre, G. Malpuech, and J. Bloch, "Spontaneous formation of a polariton condensate in a planar GaAs microcavity," Appl. Phys. Lett. **95**(5), 051108 (2009).
23. V. Kulakovskii, A. Larionov, S. Novikov, S. Höfling, C. Schneider, and A. Forchel, "Bose-Einstein condensation of exciton polaritons in high-Q planar microcavities with GaAs quantum wells," JETP Lett. **92**(9), 595–599 (2010).
24. C. W. Lai, N. Y. Kim, S. Utsunomiya, G. Roumpos, H. Deng, M. D. Fraser, T. Byrnes, P. Recher, N. Kumada, T. Fujisawa, and Y. Yamamoto, "Coherent zero-state and pi-state in an exciton-polariton condensate array," Nature **450**(7169), 529–532 (2007).
25. C. Ciuti, V. Savona, C. Piermarocchi, A. Quattropani, and P. Schwendimann, "Role of the exchange of carriers in elastic exciton-exciton scattering in quantum wells," Phys. Rev. B **58**(12), 7926–7933 (1998).
26. P. Senellart, J. Bloch, B. Sermage, and J. Y. Marzin, "Microcavity polariton depopulation as evidence for stimulated scattering," Phys. Rev. B **62**(24), R16263 (2000).
27. S. Azzini, D. Gerace, M. Galli, I. Sagnes, R. Braive, A. Lemaître, J. Bloch, and D. Bajoni, "Ultra-low threshold polariton lasing in photonic crystal cavities," Appl. Phys. Lett. **99**(11), 111106 (2011).
28. B. Zhang, Z. Wang, S. Brodbeck, C. Schneider, M. Kamp, S. Hofling, and H. Deng, "Zero-dimensional polariton laser in a subwavelength grating-based vertical microcavity," Light Sci. Appl. **3**(1), e135 (2014).
29. J.-S. Tempel, F. Veit, M. Aßmann, L. E. Kreilkamp, A. Rahimi-Iman, A. Löffler, S. Höfling, S. K. Reitzenstein, L. Worschech, A. Forchel, and M. Bayer, "Characterization of two-threshold behavior of the emission from a GaAs microcavity," Phys. Rev. B **85**(7), 075318 (2012).
30. L. S. Dang, D. Heger, R. André, F. Bœuf, and R. Romestain, "Stimulation of polariton photoluminescence in semiconductor microcavity," Phys. Rev. Lett. **81**(18), 3920–3923 (1998).
31. G. Roumpos, W. H. Nitsche, S. Höfling, A. Forchel, and Y. Yamamoto, "Gain-induced trapping of microcavity exciton polariton condensates," Phys. Rev. Lett. **104**(12), 126403 (2010).
32. L. Ferrier, E. Wertz, R. Johne, D. D. Solnyshkov, P. Senellart, I. Sagnes, A. Lemaître, G. Malpuech, and J. Bloch, "Interactions in confined polariton condensates," Phys. Rev. Lett. **106**(12), 126401 (2011).
33. U. Mohideen, R. E. Slusher, F. Jahnke, and S. W. Koch, "Semiconductor microlaser linewidths," Phys. Rev. Lett. **73**(13), 1785–1788 (1994).
34. W. H. Wang, S. Ghosh, F. M. Mendoza, X. Li, D. D. Awschalom, and N. Samarth, "Static and dynamic spectroscopy of AlGaAs/GaAs microdisk lasers with interface fluctuation quantum dots," Phys. Rev. B **71**(15), 155306 (2005).
35. D. Bajoni, P. Senellart, E. Wertz, I. Sagnes, A. Miard, A. Lemaître, and J. Bloch, "Polariton laser using single micropillar GaAs-GaAlAs semiconductor cavities," Phys. Rev. Lett. **100**(4), 047401 (2008).
36. D. M. Whittaker and P. R. Eastham, "Coherence properties of the microcavity polariton condensate," Eur. Phys. Lett. **87**(2), 27002 (2009).
37. J. Kasprzak, M. Richard, A. Baas, B. Deveaud, R. André, J.-P. Poizat, and S. Dang, "Second-order time correlations within a polariton Bose-Einstein condensate in a CdTe microcavity," Phys. Rev. Lett. **100**(6), 067402 (2008).
38. A. Rahimi-Iman, A. V. Chernenko, J. Fischer, S. Brodbeck, M. Amthor, C. Schneider, A. Forchel, S. Höfling, S. Reitzenstein, and M. Kamp, "Coherence signatures and density-dependent interaction in a dynamical exciton-polariton condensate," Phys. Rev. B **86**(15), 155308 (2012).
39. S. M. Ulrich, C. Gies, S. Ates, J. Wiersig, S. Reitzenstein, C. Hofmann, A. Löffler, A. Forchel, F. Jahnke, and P. Michler, "Photon statistics of semiconductor microcavity lasers," Phys. Rev. Lett. **98**(4), 043906 (2007).
40. T. Espinosa-Ortega and T. C. H. Liew, "Complete architecture of integrated photonic circuits based on and and not logic gates of exciton polaritons in semiconductor microcavities," Phys. Rev. B **87**(19), 195305 (2013).

#224863 - $15.00 USD Received 15 Oct 2014; revised 11 Nov 2014; accepted 11 Nov 2014; published 8 Dec 2014

1. Introduction

Microcavity exciton polaritons are quasi-particles which form in the strong coupling regime as a mixture of matter excitation and cavity photons [1]. Because of their small effective mass and their bosonic nature they can form a dynamic condensate at elevated temperatures. Such a condensate is characterized both by its spatial as well as temporal coherence of the emitted photons. Hence the light radiated from the condensate shares many similarities with a conventional photon laser. However, in strong contrast to a conventional photon laser, which relies on strong out of equilibrium conditions, a polariton laser can be operated closer to thermal equilibrium. This indicates the possibility to reduce the threshold power consumption [2, 3]. The effect of polariton lasing has been shown for different materials [4, 5], even up to room temperature in wide bandgap GaN [6], and organic [7–9] materials under optical pumping. Furthermore, polariton diodes can be excited electrically in GaAs based vertically emitting microcavities [10–12]. It is worth mentioning, that it turned out to be challenging to observe polariton laser operation or condensation effects in GaAs based microcavities with implemented InGaAs quantum wells (QWs). However, InGaAs/GaAs QW microcavities bear several significant advantages compared to GaAs/Al(Ga)As QW cavities: a) as discussed in [10–12], electrical current injection is much easier due to smaller resistivity of both the doped distributed Bragg reflectors (DBR) and the typically intrinsic cavity; b) the DBRs can be composed of the binary compounds GaAs and AlAs which have the largest possible refractive index difference of the commonly used quasi lattice matched materials on GaAs substrate. Such mirrors are inherently easier to grow, are less afflicted to detrimental roughening, hence allowing to obtain large Q-factors much easier than DBRs based on ternary AlGaAs alloys ; c) the substrate is transparent at the emission frequency, which makes transmission studies straight forward, being particularly appealing in resonant studies; d) compared to GaAs QWs, InGaAs QWs allow for a significantly higher flexibility in the design of the QW bandstructure. Consequently, the strain environment (hence the splitting between heavy hole and light holes), the emission wavelength, the oscillator strength and the tuning behavior in electric (via the quantum confined Stark effect) and magnetic fields can be conveniently adjusted via the QW thickness and the composition of the alloy [13–16]. In fact, it is possible to tune the wavelength band between 830 nm and 1200 nm, which is in particular appealing from the application point of view; e) InGaAs QWs have significantly larger exciton g-factors compared to GaAs/AlGaAs QWs [16], making them very interesting candidates to observe pronounced spinor polariton effects in a magnetic field [17]. These points make polariton lasers (i.e non-resonantly injected polariton condensates) based on InGaAs QWs, in addition to their resonantly driven counterparts [18, 19] highly desirable. In this work we provide evidence for optically injected polariton lasing in a device based on AlAs/GaAs DBRs sandwiching an intrinsic GaAs cavity with four embedded InGaAs QWs. Additionally, we demonstrate that we can switch between the polartion lasing in the strong coupling regime and the cavity mediated lasing in the weak coupling regime by applying a voltage to the microcavity.

2. Sample design and experimental setup

The layer structure of the microresonator consists of 23(27) doped AlAs/GaAs mirrorpairs which is schematically shown in Fig. 1(a) and it has been described in detail by Schneider et al in [11]. The typical normal mode splitting which is a signature of the strong coupling regime was mapped out in the photoreflection geometry, yielding a Rabi splitting of 5.5meV. Despite the high Indium content of 15% in the QWs, we can measure an inhomogeneous broadening of the four integrated QWs, which is as low as 2.7 meV. For these standard macro photoluminescence measurements, we removed the top DBR segment via reactive ion etching. Micropillar cavities with diameters of 20μm were etched into the layer structure, and the sample was planarized by benzocyclobuthene.

#224863 - $15.00 USD Received 15 Oct 2014; revised 11 Nov 2014; accepted 11 Nov 2014; published 8 Dec 2014

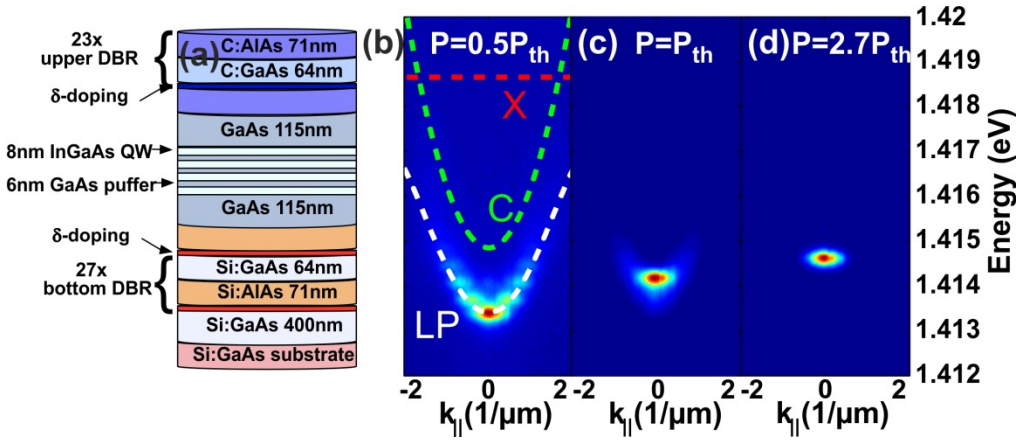

Fig. 1. (a) Scheme of used structure. False colour energy dispersions for (b) lower polariton with mode patern caused by 20μm confinement (c) polariton condensate at the threshold with dispersion in the background and (d) condensate three times above the threshold with emission from k = 0.

Afterwards, electrical contacts were evaporated on the backside of the Si-doped GaAs wafer and the top of the micropillar to enable one to apply a voltage to the device. In our experiment, we chose a detuning between the exciton and photon mode of –3.7meV. For optical excitation a pulsed laser with a pulse length of 50ps and repetition rate of 82MHz is used. It is set to the energy of the first Bragg minimum, about 110meV above the polaritonic resonances. Hot excitons, which can relax via phonon interactions and form polaritons, are created inside the microcavity. The relaxation process continues till the energy difference between exciton and photon is in the order of the Rabi-splitting. This makes the photonic component notable and shortens the polaritonic lifetime. At high densities, polariton-polariton interaction gives rise to a new relaxation channel, which facilitates the formation of a macroscopically occupied ground state. Further general information on the formation of polariton condensates can for example be found in [20]. Details on the relaxation pathway in this structure will be published elsewhere [21]. All experiments were performed at a temperature of 6K. An external voltage of 1.3 V was applied to the sample to reach flat band conditions, except for the electro-optical studies presented in this manuscript. Throughout the paper all threshold values refer to flatband condition. Because of the high Q-factor of around 6300, polaritons can cool into the bottom of the lower polariton branch, which features a parabolic dispersion with an effective mass of $4.4\ 10^{-5}\ m_e$ with m_e as the electron mass. In agreement with other reports on high-Q microcavities in the strong coupling regime, the upper polariton branch as well as higher excited states of the lower branch are depleted as a result of this process [22, 23].

#224863 - $15.00 USD Received 15 Oct 2014; revised 11 Nov 2014; accepted 11 Nov 2014; published 8 Dec 2014

3. Experimental results

3.1 Polariton lasing characteristics

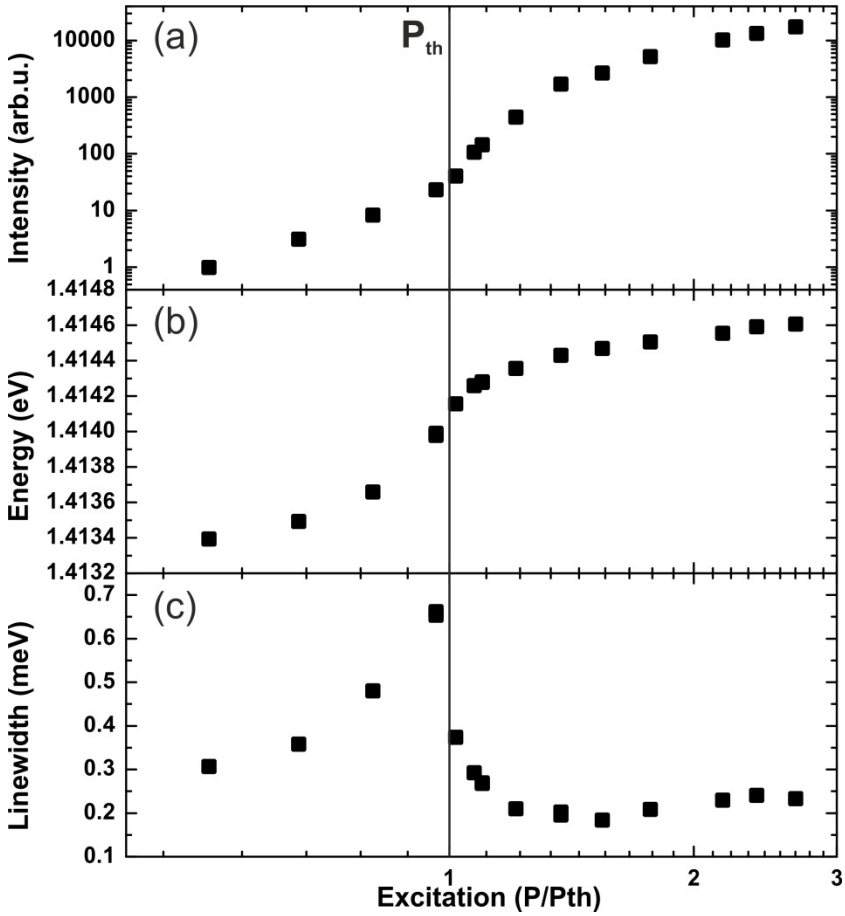

Fig. 2. Excitation power dependence of (a) the integrated ground state intensity of k = 0 ± 0.1 μm^{-1} (b) the ground state emission energy and (c) the linewidth. The threshold is characterized by a non-linearity, stronger energy shift and drop of linewidth.

The in-plane polariton dispersion is collected with a far field spectroscopy setup [24]. The recorded contour plots are presented in Fig. 1 for different excitation powers. The lower polariton mode at $0.5*P_{th}$ in Fig. 1(b) shows a mode pattern along the dispersion because of the lateral confinement of 20μm originating from the micropillar geometry. The uncoupled exciton (red broken line) and photon (green broken line) are plotted with the resulting lower polariton fit (white broken line). With increasing excitation power the emission is shifted to higher energy because of exciton-exciton-interactions [25] with its polaritonic dispersion being still visible in the background in Fig. 1(c). Almost three times above threshold (which corresponds to a power density of 620 W/cm^2) in Fig. 1(d) the dispersion is not observable anymore and the emission is centered around k = 0 approximately 0.4meV below the bare cavity mode. In order to characterize the behavior in more detail the emission of k = 0 ± 0.1 μm^{-1} was integrated and fitted by a Lorentzian lineshape. The evolution of characteristic parameters with increasing excitation power is shown in Fig. 2. The input-output-characteristic in Fig. 2(a) shows a quadratic behavior for small excitation [26–28] and a strong non-linearity at the threshold, which coincides with a change in the dispersion. Above $1.5*P_{th}$ the slope changes again. We note that a second non-linearity, which commonly is attributed to

#224863 - $15.00 USD Received 15 Oct 2014; revised 11 Nov 2014; accepted 11 Nov 2014; published 8 Dec 2014

the onset of conventional lasing [29, 30], cannot be reached since heating effects set in before this transition can be crossed. As we will show later in this manuscript, the transition to the weak coupling, however, gets accessible via manipulation of the intrinsic electric field. The energy at k = 0 is shown in Fig. 2(b): It continuously shifts towards higher energy because of particle interactions. Around threshold the slope changes from linear to logarithmic in good agreement with previous reports on GaAs based polariton lasers [31, 32]. The change of emission energy above the threshold is a hint for the preservation of strong coupling. The laser emission from the cavity mode is typically pinned for all excitation powers, except for minor deviations caused by a carrier dependent refractive index [29, 33] or heating [34]. The linewidth in Fig. 2(c) shows an increase from 0.31meV in the linear regime to 0.65meV just below the threshold caused by polariton-polariton-interactions, which has been observed in most GaAs based polariton lasers [29, 35]. At threshold, the linewidth is subject to a sudden drop as a result of temporal coherence in the condensate to a minimum value of 0.18meV around $1.5*P_{th}$. Number fluctuations and inter-particle interactions inside the condensate subsequently lead to decoherence and therefore a rise of the linewidth above $1.5*P_{th}$ [36].

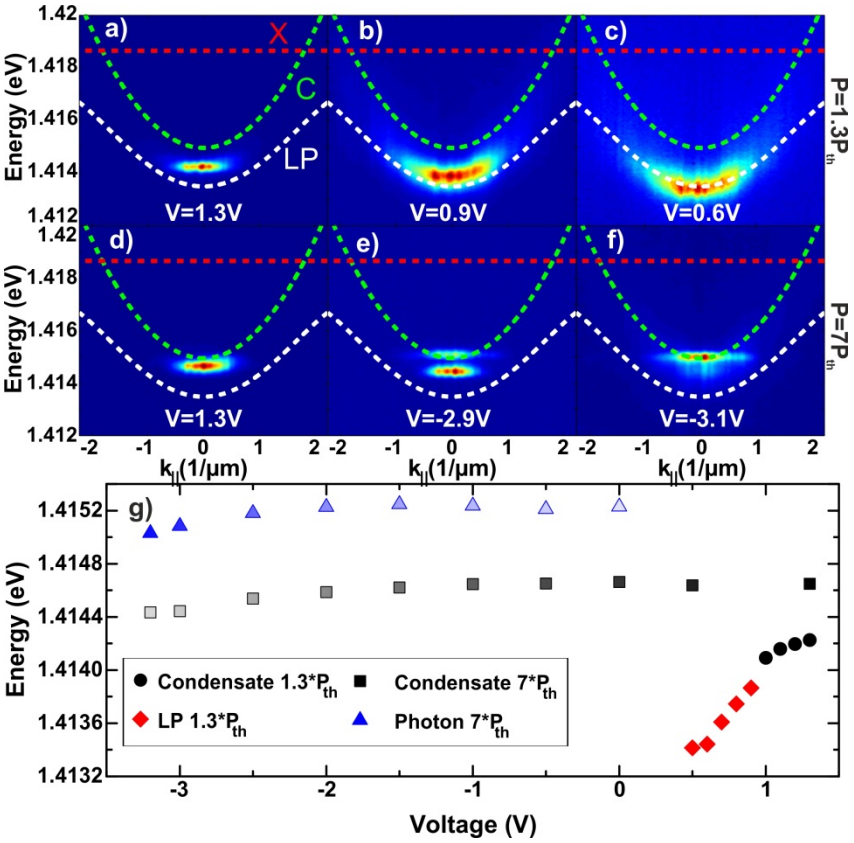

Fig. 3. Energy dispersions for an excitation of $1.3*P_{th}$ with an applied Voltage of (a)1.3V (equals flatband condition) (b) 0.9V and (c) 0.6V. As the bandstructure is tilted the condensate is destroyed and normal polariton emission sets in. Energy dispersions for an excitation of $7*P_{th}$ with an applied Voltage of (d)1.3V (equals flatband condition) (e) –2.9V and (f) –3.1V. The electric field breaks the strong coupling regime and emission jumps to the photon mode. (g) Energy vs. voltage to further demonstrate the loss of the condensate regime. Markers filling visibility for $7*P_{th}$ visualizes the emission intensity.

#224863 - $15.00 USD Received 15 Oct 2014; revised 11 Nov 2014; accepted 11 Nov 2014; published 8 Dec 2014

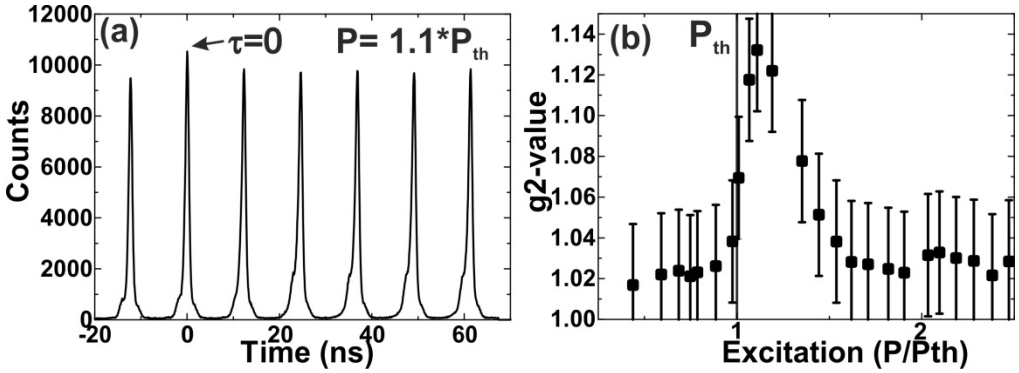

Fig. 4. (a) Exemplary $g^{(2)}(\tau)$ measurement slightly above threshold. (b) Excitation power dependence of the $g^{(2)}(\tau = 0)$ value with an increase around the threshold.

3.2 Electro-optical switching

We will now extend our study and investigate the electro-optical properties of our polariton condensate. First, we drive the polariton condensate slightly above the threshold for polariton lasing, as shown in Fig. 3(a) ($1.3*P_{th}$, corresponding to 2.2 mW). Under these conditions, already minor deviations from the flatband conditions result in increased losses via carrier tunneling out of the QWs. This is causing a decrease of the carrier capturing rate in the QWs due to the built-in electric field which drags the injected carriers to the DBR segments. Consequently, the effective injection rate decreases with an applied voltage lower than flatband condition. Therefore the condensate threshold density can no longer be reached, and the emission is expected to follow the lower polariton branch. This scenario is directly reflected in Figs. 3(b) and 3(c). For even stronger tilted bands, one would expect a transition to the weak coupling regime resulting from electrostatic quenching of the exciton oscillator strength and fast tunneling losses exceeding the Rabi frequency. This scenario is shown in Figs. 3(d)-3(f). Here, in order to ensure a sufficiently strong photoluminescence signal even in the tunnel current regime, we drive the condensate 7 times above flatband threshold.

Once an internal voltage of −2.9 V is reached, along with a redshift of the condensate as a result of the quantum confined stark effect, we observe the appearance of a second mode in the emission spectrum. This feature is blueshifted with respect to the condensate and located on the emission energy of the uncoupled cavity resonance. Further increasing the reverse bias to −3.1 V, the condensate related emission is vanished, and only the emission from the bare cavity mode persists. This leads us to the interpretation that the strong coupling is lost under these conditions, and the system enters the weak coupling regime. This is visualized in more detail in Fig. 3(g), which shows the emission energy dependence on the applied voltage. One notes that far above threshold both, the condensate and the photon mode are recorded, which we attribute to the time integration of different regimes caused by the pulsed excitation. The intensity of the two modes show oppositional behavior as the condensate diminishes and the photon mode brightens while applying a stronger reverse bias. This is visualized with the visibility of the markers fillings.

3.3 Photon statistics

To investigate the temporal coherence of the emission from the condensate in greater detail, we characterize our system via photon statistic measurements. The second order correlation function is defined as $g^{(2)}(\tau) = \langle I(t+\tau)I(t)\rangle / (\langle I(t)\rangle\langle I(t+\tau)\rangle$ with I(t) as the emission intensity at time t and $\langle..\rangle$ as time average. We record $g^{(2)}(\tau = 0)$ values with a Hanbury Brown and Twiss setup using avalanche photo diodes with a time resolution of 400ps [4, 37, 38]. Therefore the dispersion ground state was filtered by a monochromator with an energy

#224863 - $15.00 USD Received 15 Oct 2014; revised 11 Nov 2014; accepted 11 Nov 2014; published 8 Dec 2014

resolution of about 0.2meV. The $g^{(2)}(\tau = 0)$ value is calculated as the ratio between the area of the τ = o peak N_0 and the mean value of the area of n $\tau \neq$ o peaks $\overline{N_S} = N_S / n : g^2(\tau = 0) = \frac{N_0}{\overline{N_S}}$. The error Δg^2 is calculated via Gaussian error propagation: $\Delta g^2 = \sqrt{\left(\frac{1}{\overline{N_S}}\right)^2 * N_0^2 + \left(\frac{N_0}{\overline{N_s^2}}\right)^2 * \overline{N_s^2}}$. With the onset of temporal coherence in the condensate, a drop from $g^{(2)}(\tau = 0) = 2$ (characteristic for thermal light) to $g^{(2)}(\tau = 0) = 1$ (coherent light) is expected. An exemplary result in Fig. 4(a) recorded slightly above threshold clearly shows a notably increased τ = 0 peak, as a signature of an enhanced two photon probability in this regime. The power dependent evolution of the $g^{(2)}(\tau = 0)$ function is plotted in Fig. 4(b). We clearly observe a drop of the $g^{(2)}(\tau = 0)$ function towards 1 with increasing pump power, indicating coherent emission from our polariton laser. For small powers, in contrast to the expected behavior, the $g^{(2)}(\tau = 0)$ value again approaches 1. This is a direct consequence of the finite temporal resolution of our detectors, which significantly exceeds the coherence times of a thermal emitter [39]. It is worth noting, that the sudden drop in the coherence function to a value close to 1 is in contrast to previous studies of the second order temporal correlation in extended two-dimensional polariton systems [4, 29, 37, 38]. A comparably slow decrease above threshold was observed, supposedly as a consequence of polariton scattering from the ground-state to higher states at $k \neq 0$ [4]. The micropillar geometry of our system, however, strongly reduces the available states at finite k values, which efficiently leads to a suppression of this unfavorable effect, resulting in enhanced temporal coherence in our polariton laser.

4. Conclusion

In conclusion we have shown evidence for polariton laser operation under optical excitation in a cavity with embedded InGaAs quantum wells. The polariton laser is manifested by its distinct far field emission characteristics. It features a pronounced non-linearity in the input-output-characteristic and a persisting blueshift above the threshold. Temporal coherence is reflected by the drop of the emission linewidth at threshold and in the second order correlation function around threshold. We furthermore establish electro-optical switching from the linear regime to the condensate, as well as from the condensate to the weak coupling regime, as well as electro-optical tuning of the condensate. We anticipate that our experiment can be directly extended to compact, integrated electro-optical polaritonic experiments and functional devices due to the doped and contacted microcavity. For example the realization of tunable circuits, switches logic devices [40], and eventually electro-optically tunable polariton traps which can be exploited in polaritonic quantum simulation.

Acknowledgments

The authors thank A. Wolf, M. Emmerling and M. Lermer for assistance in sample preparation, A. Rahimi-Iman for his initial contributions to the experiment, and P. Lagoudakis for vivid discussions. Financial support by the State of Bavaria is gratefully acknowledged. This publication was funded by the German Research Foundation (DFG) and the University of Wuerzburg in the funding programme Open Access Publishing.